European Journal of Mechanics / B Fluids 77 (2019) 162–170

Contents lists available at ScienceDirect

European Journal of Mechanics / B Fluids

journal homepage: www.elsevier.com/locate/ejmflu

Virtual wave stress and transient mean drift in spatially damped long interfacial waves

Jan Erik H. Weber [a,*], Kai H. Christensen [a,b]

[a] Department of Geosciences/MetOs, University of Oslo, PO Box 1022, Blindern, NO-0315 Oslo, Norway
[b] Norwegian Meteorological Institute, PO Box 43, Blindern, NO-0313 Oslo, Norway

ARTICLE INFO

Article history:
Received 9 October 2018
Received in revised form 1 February 2019
Accepted 8 April 2019
Available online 14 April 2019

ABSTRACT

The mean drift in spatially damped long gravity waves at the boundary between two layers of immiscible viscous fluids is investigated theoretically by applying a Lagrangian description of motion. The focus of the paper is on the development of the drift near the interface. The initial drift (inviscid Stokes drift + viscous boundary-layer terms) associated with the instantaneously imposed wave field does not generally fulfill the conditions at the common boundary between the layers. Hence, transient Eulerian mean currents develop on both sides of the interface to ensure continuity of velocities and viscous stresses. The development of strong jet-like Eulerian currents increasing with time in this problem is related to the action of the virtual wave stress (VWS). Very soon (after a few wave periods) the transient Eulerian part dominates in the Lagrangian mean current. This effect is similar to that found for the drift in short gravity waves with a film-covered surface. A new relation is derived showing that the difference between the VWS's at the interface is given by the divergence of the total horizontal wave momentum flux in a two-layer system. Our analysis with spatially damped waves also yields the Lagrangian change of the mean surface level and mean interfacial level (the divergence effect) due to periodic baroclinic wave motion.

1. Introduction

When the wave amplitude in progressive surface waves attenuates due to friction in the fluid, mean momentum is transferred from the waves to Eulerian mean currents through the action of the virtual wave stress (hereafter VWS), and denoted by τ_w. The concept of VWS was first introduced by Longuet-Higgins [1] to explain this redistribution of mean horizontal momentum in a viscous fluid. For temporally damped waves Longuet-Higgins showed by integrating in time that $\int_0^\infty \tau_w dt = M_0$, where M_0 is the initial total wave momentum. For spatially damped surface waves Weber [2] related the VWS to the divergence of the wave momentum flux. His result is valid whether the surface is uncontaminated (clean) or covered by a thin film. For spatially damped surface waves the action of the VWS leads to Eulerian mean currents that grow in time, as demonstrated in [2]. In particular, when the surface is contaminated (film covered), the VWS is greatly enhanced, leading to Eulerian mean currents that becomes stronger than the Stokes drift in a relatively short time interval; see e.g. [3]. The large increase in surface drift in the presence of an inextensible film was originally demonstrated in [4] from vorticity considerations. Recent high quality measurements also reveal the effect of viscosity on the near-surface wave-induced drift, as shown in [5].

Analogous to the situation at the surface, the VWS must act at the boundary between two immiscible fluids of different densities and viscosities, and the main aim of the present paper is to investigate the importance of VWS on the drift in interfacial waves. To facilitate this task, we pose the interfacial wave problem as simple as possible so the basic physics is not lost in mathematical details. Particularly, in the study of long progressive interfacial waves we assume that the density difference across the interface is small, but the layers may have substantially different viscosities. The respective layer depths may also vary in an arbitrary sense. The only requirement is that the wavelength must be much larger than the depth of each layer (the shallow water approximation). We use an Eulerian framework for defining the problem, because this approach is familiar to most readers. To obtain the wave-induced drift, we switch to a Lagrangian description of motion. Then we can allow for interfacial wave amplitudes that are much larger than the thickness of the viscous boundary layers.

The study of the drift in gravity waves in a two-layer setting with different densities and viscosities is not new. In an Eulerian formulation this problem was analyzed by Dore [6–9] for undamped waves, applying a double-boundary layer method with matched asymptotic expansions. Using Dore's technique, Wen

* Corresponding author.
E-mail addresses: j.e.weber@geo.uio.no (J.E.H. Weber), kaihc@met.no (K.H. Christensen).

https://doi.org/10.1016/j.euromechflu.2019.04.004

& Liu [10] extended his analysis to temporally damped waves. Applying a direct Lagrangian approach Weber and Førland [11] considered the drift in short temporally and spatially attenuated waves in an air–water system. Later Piedra-Cueva [12] studied the steady two-layer problem in the Lagrangian formulation with emphasis on transport in a very viscous (mud) bottom layer induced by spatially damped surface water waves. A similar problem for the steady drift in partial standing surface waves in a two-layer viscous system was investigated in [13], also using a direct Lagrangian approach.

We assume that our wave field attenuate in space due to friction. This is particularly relevant to experiments in wave tanks with a wave generator operating at a given frequency at one end of the tank. Most studies of this problem consider the final steady state. The exception is the transient problem studied in [10], but because they consider temporally damped waves, their Eulerian mean currents die out in time. In our case, with spatially attenuated waves, the VWS leads to the generation of Eulerian mean currents near the interface that always increase in time. We will therefore pay particular attention to the early stages of the development of the drift currents in this paper. Concerning the relevance to wave tank experiments, this means that we consider time scales comparable to the typical duration of a wave tank experiment before adverse mean pressure gradients are set up, and a steady pattern with re-circulating flow is established.

The use of the Lagrangian formalism yields directly the Lagrangian change of mean surface level and interfacial level associated with periodic baroclinic waves. Similar Lagrangian changes of the mean surface level for short gravity waves have been reported in [14,15].

The rest of this paper is organized as follows: In Section 2 we formulate the problem mathematically, using the familiar Eulerian description of motion, and applying the long-wave assumption. In Section 3 we switch to a Lagrangian formulation, deferring the trivial linear solutions to the Appendix. The Lagrangian equations for the mean drift are given in Section 4, while the Lagrangian mean level changes due to interfacial waves are derived in Section 5. In Section 6 we consider the particular solutions to the wave drift problem, and in Section 7 we discuss the wave-induced Eulerian mean flow and the action of the VWS. In Section 8 we discuss the role of VWS in the mean momentum balance, and in Section 9 we present case studies showing how the Lagrangian mean drift varies with viscosity differences and depth ratios in the two layers. In Section 10 we outline a simple laboratory experiment for verifying the theoretical results of this paper, and Section 11 contains a short discussion and some final remarks.

2. Mathematical formulation

We study the wave motion in a system of two horizontal incompressible fluid layers, denoting upper and lower layer variables by subscripts 1 and 2, respectively. When undisturbed, the layers have constant depths H_1 and H_2. The corresponding constant densities and viscosities are ρ_1, ν_1, and ρ_2, ν_2, respectively. We let the horizontal x axis be situated at the undisturbed interface, and the z axis is positive upward. To make this study as simple as possible without losing the basic physics, we consider two-dimensional motion in a non-rotating semi-infinite domain $x \geq 0$. The material surface is given by $z = H_1 + \eta(x, t)$, where t denotes time, and the interface is given by $z = \xi(x, t)$. The respective unit vectors are given by $(\boldsymbol{i}, \boldsymbol{k})$, and the fluid velocity vector is $\boldsymbol{v} = (u, w)$.

We take that the waves are so long that we can make the hydrostatic approximation in the vertical direction. Neglecting the presence of an external pressure at the surface, we may then write for the pressure in the two layers

$$p_1 = -\rho_1 g z + \rho_1 g\,(H_1 + \eta) \tag{2.1}$$

$$p_2 = -\rho_2 g z + g\,(\rho_2 - \rho_1)\,\xi + \rho_1 g (H_1 + \eta) \tag{2.2}$$

where g is the acceleration due to gravity. The horizontal momentum equations in an Eulerian formulation then become:

$$D_t u_1 = -g\eta_x + \nu_1 u_{1zz} \tag{2.3}$$

$$D_t u_2 = -g\frac{(\rho_2 - \rho_1)}{\rho_2}\xi_x - g\frac{\rho_1}{\rho_2}\eta_x + \nu_2 u_{2zz}. \tag{2.4}$$

Here, subscripts denote partial differentiation, and $D_t \equiv \partial/\partial t + \boldsymbol{v}\cdot\nabla$ is the material derivative following a fluid particle. In the viscous terms we have assumed that $\left|\partial^2/\partial z^2\right| \gg \left|\partial^2/\partial x^2\right|$. Finally, from volume conservation:

$$u_{1,2x} + w_{1,2z} = 0, \tag{2.5}$$

where subscripts 1,2 refer to upper and lower layer, respectively. From (2.5) one finds, by applying the nonlinear kinematic boundary conditions, the well-known exact relations

$$\eta_t - \xi_t = -\left(\int_{\xi}^{H_1+\eta} u_1 dz\right)_x \tag{2.6}$$

$$\xi_t = -\left(\int_{-H_2}^{\xi} u_2 dz\right)_x. \tag{2.7}$$

The stresses in the fluid must be continuous across the interface. In the present hydrostatic formulation the pressure fulfills this condition in the normal direction; see (2.1)–(2.2). We denote the external horizontal stresses on both sides of the material interface $z = \xi(x, t)$ by $\tau_{1,2}^{(x)}$, where

$$\tau_{1,2}^{(x)} = \rho_{1,2}\nu_{1,2}\left(u_{1,2z} + w_{1,2x}\right) + p_{1,2}\xi_x - 2\rho_{1,2}\nu_{1,2}u_{1,2x}\xi_x. \tag{2.8}$$

Continuity of horizontal stresses implies that $\tau_1^{(x)} = \tau_2^{(x)}$ at $z = \xi(x, t)$. Utilizing that $p_1 = p_2$ from (2.1)–(2.2), and applying the long wave assumption $\left|w_{1,2x}\right| \ll \left|u_{1,2z}\right|$, we find that

$$\rho_1\nu_1\,(u_{1z} - 2u_{1x}\xi_x) = \rho_2\nu_2\,(u_{2z} - 2u_{2x}\xi_x)\,, \quad z = \xi(x, t). \tag{2.9}$$

Furthermore, the velocities must be continuous at the interface, i.e.

$$u_1 = u_2,\, w_1 = w_2, \quad z = \xi(x, t). \tag{2.10}$$

3. Lagrangian analysis

The Eulerian formulation in the previous section provides the most familiar tool for studying wave problems. However, since we here must incorporate thin viscous boundary layers at the wavy interface, the Cartesian Eulerian approach actually requires that the wave amplitude is smaller than the boundary-layer thicknesses, which limits the wave amplitude quite severely; see e.g. [4]. To remedy this one could use curvilinear coordinates, following the wavy interface, but this is problematic since the wave amplitude in our problem attenuates in space. A better option is to use particle-following Lagrangian coordinates. Then the interfacial amplitude can be arbitrary large (but small enough for linearization to be valid).

In this description independent particle coordinates for two-dimensional flow are denoted by (a, c), and the particle positions can be written $X = X(a, c, t)\,, Z = Z(a, c, t)$. Velocity and acceleration components become (X_t, Z_t) and (X_{tt}, Z_{tt}), respectively. One of the advantages of this formulation is that the material

surface and material interface are given at all times by $c = H_1$, and $c = 0$.

Mass (actually volume) conservation in each layer can be expressed as, [16]:

$$J(X, Z) = J(X_0, Z_0) \tag{3.1}$$

Here $X_0 = X(a, c, t = 0)$, and $Z_0 = Z(a, c, t = 0)$ are the initial particle positions. Furthermore,

$$J(F, G) = F_a G_c - F_c G_a \tag{3.2}$$

is the Jacobian operator. Formally, the positions and the pressure P in each layer can be written as

$$\left.\begin{aligned} X &= a + x\,(a, c, t) \\ Z &= c + z\,(a, c, t) \\ P &= p_0 - \rho g c + p(a, c, t) \end{aligned}\right\} \tag{3.3}$$

where p_0 is a constant. The continuity equation in each layer now becomes from (3.1):

$$x_a + z_c + J(x, z) = x_{0a} + z_{0c} + J(x_0, z_0) \tag{3.4}$$

In (3.3) x, z, and p may be expanded after the small dimensionless parameter ε defined as

$$\varepsilon = A/H_1, \tag{3.5}$$

see e.g. [17]. Here A is the interfacial wave amplitude in the wave generation area. Then

$$\left.\begin{aligned} \left(x_{1,2}, z_{1,2}\right) &= \varepsilon \left[x_{1,2}^{(1)}, z_{1,2}^{(1)}\right] + \varepsilon^2 \left[x_{1,2}^{(2)}, z_{1,2}^{(2)}\right] + \cdots \\ \eta &= \varepsilon \eta^{(1)} + \varepsilon^2 \eta^{(2)} + \cdots \\ \xi &= \varepsilon \xi^{(1)} + \varepsilon^2 \xi^{(2)} + \cdots \end{aligned}\right\} \tag{3.6}$$

To $O(\varepsilon)$ we have from (3.4) that $x_{1,2ta} + z_{1,2tc} = 0$. Hence for a progressive wave proportional to $\exp(-i\omega t)$, we must have that $x_a + z_c = 0$ in each layer. It then follows from (3.4) that $x_{0a} + z_{0c} = 0$ to this order. Accordingly, for the continuity (3.1) in each layer we have:

$$J(X_0, Z_0) = 1 + O(\varepsilon^2) \tag{3.7}$$

In the transformation of the momentum equations (2.3)–(2.4) from Eulerian to Lagrangian form, we change the Eulerian notation for the independent spatial coordinates to capital letters X, Z. In Lagrangian description, these positions are functions of the independent Lagrangian variables a, c, t, as explained before. For a function F the relation between the spatial Eulerian partial derivatives and the Lagrangian derivatives is; see e.g. [18]:

$$\left.\begin{aligned} F_X &= J(F, Z)/J(X, Z) \\ F_Z &= J(X, F)/J(X, Z) \end{aligned}\right\} \tag{3.8}$$

where the Jacobian operator is defined by (3.2). From (3.1) and (3.7) we notice that $J(X, Z) = 1 + O(\varepsilon^2)$. Hence by introducing the Lagrangian deviations x, z from (3.3), we find, correct to second order:

$$\left.\begin{aligned} F_X &= F_a + J(F, z) \\ F_Z &= F_c + J(x, F) \\ F_{ZZ} &= F_{cc} + 2J(x, F_c) + J(x_c, F) \end{aligned}\right\} \tag{3.9}$$

Furthermore, in this problem we assume that the density difference between the layers is so small that we can take

$$\rho_2 - \rho_1 = \Delta\rho, \quad \rho_1 \approx \rho_2 = \rho \tag{3.10}$$

Utilizing (3.9), we obtain to $O(\varepsilon^2)$ for the horizontal momentum equations (2.3)–(2.4):

$$x_{1tt} = -g\eta_a(1 + z_{1c}) + \nu_1 \left[x_{1tcc} + 2J(x_1, x_{1tc}) + J(x_{1c}, x_{1t})\right] \tag{3.11}$$

$$x_{2tt} = -\left[g_*\xi_a + g\eta_a\right](1 + z_{2c}) + \nu_2 \left[x_{2tcc} + 2J(x_2, x_{2tc}) + J(x_{2c}, x_{2t})\right] \tag{3.12}$$

where g_* is the reduced gravity defined by

$$g_* = g\Delta\rho/\rho \tag{3.13}$$

The linear (periodic) wave problem to $O(\varepsilon)$ is trivial, and we have deferred the details to the Appendix. Here, the linear solutions are marked by a tilde.

4. The Lagrangian equations for the mean drift

With reference to (3.6), we define nonlinear mean quantities:

$$\overline{u}_1 = \varepsilon^2 \overline{x_{1t}^{(2)}}, \; \overline{u}_2 = \varepsilon^2 \overline{x_{2t}^{(2)}}, \tag{4.1}$$

$$\overline{\eta} = \varepsilon^2 \overline{\eta^{(2)}}, \; \overline{\xi} = \varepsilon^2 \overline{\xi^{(2)}}, \tag{4.2}$$

where the overbar denotes average over one wave period, and ε is given by (3.5). The equations for mean flow to $O(\varepsilon^2)$ in the upper and lower layer becomes from (3.11) and (3.12), respectively:

$$\begin{aligned} \nu_1 \overline{u}_{1cc} - \overline{u}_{1t} = \nu_1 \Big(&2\overline{\tilde{x}_{1tac}\tilde{x}_{1c}} + \overline{\tilde{x}_{1cc}\tilde{x}_{1ta}} - 2\overline{\tilde{x}_{1tcc}\tilde{x}_{1a}} - \overline{\tilde{x}_{1ac}\tilde{x}_{1tc}}\Big) \\ &+ \frac{g_* H_2}{H_1 + H_2}\overline{\tilde{\xi}_a \tilde{x}_{1a}} + g\overline{\eta}_a \end{aligned} \tag{4.3}$$

$$\begin{aligned} \nu_2 \overline{u}_{2cc} - \overline{u}_{2t} = \nu_2 \Big(&2\overline{\tilde{x}_{2tac}\tilde{x}_{2c}} + \overline{\tilde{x}_{2cc}\tilde{x}_{2ta}} - 2\overline{\tilde{x}_{2tcc}\tilde{x}_{2a}} - \overline{\tilde{x}_{2ac}\tilde{x}_{2tc}}\Big) \\ &- \frac{g_* H_1}{H_1 + H_2}\overline{\tilde{\xi}_a \tilde{x}_{2a}} + g_*\overline{\xi}_a + g\overline{\eta}_a. \end{aligned} \tag{4.4}$$

We have here utilized that $\tilde{\eta} = -(\Delta\rho/\rho)H_2\tilde{\xi}/(H_1 + H_2)$ for baroclinic motion; see (A.7). Furthermore, we have used (A.3) in the pressure terms.

At the interface $c = 0$, the stress condition (2.9) and velocity condition (2.10) become, respectively:

$$\begin{aligned} \nu_1 \overline{u}_{1c} - \nu_2 \overline{u}_{2c} = &-\nu_1 \left(\overline{\tilde{x}_{1tc}\tilde{x}_{1a}} - \overline{\tilde{x}_{1ta}\tilde{x}_{1c}} - 2\overline{\tilde{x}_{1ta}\tilde{\xi}_a}\right) \\ &+ \nu_2 \left(\overline{\tilde{x}_{2tc}\tilde{x}_{2a}} - \overline{\tilde{x}_{2ta}\tilde{x}_{2c}} - 2\overline{\tilde{x}_{2ta}\tilde{\xi}_a}\right) \end{aligned} \tag{4.5}$$

$$\overline{u}_1 = \overline{u}_2. \tag{4.6}$$

We use real values for the wave variables in (A.11)–(A.12), (A.18)–(A.19), and take that

$$\tilde{\xi} = H_1 \delta \cos(ka - \omega t) \tag{4.7}$$

where we for simplicity have introduced the slowly-varying amplitude parameter δ by

$$\delta = (A/H_1)\exp(-\alpha a). \tag{4.8}$$

Then (4.3) reduces to:

$$\begin{aligned} \overline{u}_{1cc} - \overline{u}_{1t}/\nu_1 = C_* Q_1 \gamma_1^2 \delta^2 \big[&3Q_1 \exp(-2\gamma_1 c) \\ &-4\exp(-\gamma_1 c)\sin(\gamma_1 c)\big] + \alpha C_* \gamma_1^2 \delta^2/k + g\overline{\eta}_a/\nu_1. \end{aligned} \tag{4.9}$$

Here the interfacial phase speed C_* from (A.22) is

$$C_* = \omega/k = (g_* H_1 H_2)^{1/2}/(H_1 + H_2)^{1/2}. \tag{4.10}$$

In the lower layer we find

$$\begin{aligned} \overline{u}_{2cc} - \overline{u}_{2t}/\nu_2 = h^2 C_* Q_2 \gamma_2^2 \delta^2 \big[&3Q_2 \exp(2\gamma_2 c) + 4\exp(\gamma_2 c)\sin(\gamma_2 c)\big] \\ &+ \alpha h^2 C_* \gamma_2^2 \delta^2/k + g_*\overline{\xi}_a/\nu_2 + g\overline{\eta}_a/\nu_2. \end{aligned} \tag{4.11}$$

Here we have introduced the depth ratio

$$h = H_1/H_2. \tag{4.12}$$

We recall that Q_1 and Q_2 in (4.9) and (4.11) are defined by (A.15), and the inverse Stokes boundary-layer thicknesses γ_1, γ_2 by (A.13).

5. Lagrangian mean level changes

We may split the particular solutions of (4.9) and (4.11) into c-dependent parts, and parts that do not depend on the vertical coordinate. For an infinitely long channel we disregard any build-up of the mean surface and mean interfacial levels due to mass accumulation, so the only Lagrangian mean level changes are due to the presence of waves; see e.g. [14] for surface waves.

The mean level changes in our problem are obtained from the fact that the drift velocities cannot become infinite in time. Hence, the parts of the right-hand sides of (4.9) and (4.11) that do not depend on c must vanish, i.e.

$$\alpha C_* \gamma_1^2 \delta^2/k + g\overline{\eta}_a/\nu_1 = 0, \tag{5.1}$$

and

$$\alpha h^2 C_* \gamma_2^2 \delta^2/k + g_* \overline{\xi}_a/\nu_2 + g\overline{\eta}_a/\nu_2 = 0, \tag{5.2}$$

where δ and h are defined by (4.8) and (4.12), respectively. The surface mean level then becomes from (5.1):

$$\overline{\eta} = C_*^2 \delta^2/(4g) \tag{5.3}$$

By inserting into (5.2), we find for the interfacial mean level

$$\overline{\xi} = C_*^2(h^2 - 1)\delta^2/(4g_*) \tag{5.4}$$

Since Lagrangian mean level changes basically are related to irrotational waves with a mean forward mass transport, i.e. a Stokes drift [19], we can introduce the Stokes momentum flux in (5.3) and (5.4). We may obtain the Stokes drift $\overline{u}_S$ in the long-wave limit $kH_1 \ll 1, kH_2 \ll 1$, from the derivation by Longuet-Higgins [20]. In Lagrangian notation we can write Longuet-Higgins' result to second order in wave steepness as

$$\overline{u}_S = \overline{\tilde{x}_{ta}\tilde{x}} + \overline{\tilde{x}_{tc}\tilde{z}}. \tag{5.5}$$

Inserting real parts from (A.11)–(A.12) and (A.18)–(A.19), and excluding the boundary-layer terms, one obtains in the two layers, respectively:

$$\overline{u}_{S1} = C_* \delta^2/2, \tag{5.6}$$

$$\overline{u}_{S2} = C_* h^2 \delta^2/2 \tag{5.7}$$

The corresponding Stokes volume fluxes are

$$\overline{U}_{S1} = H_1 \overline{u}_{S1}, \overline{U}_{S2} = H_2 \overline{u}_{S2}. \tag{5.8}$$

Inserting from (5.6) into (5.3) and (5.4), we obtain

$$\overline{\eta} = C_* \overline{U}_{S1}/(2gH_1), \tag{5.9}$$

and

$$\overline{\xi} = C_*(h^2 - 1)\overline{U}_{S1}/(2g_* H_1). \tag{5.10}$$

We note from (5.9) that the surface disturbance always leads to a positive change of surface level. This is in accordance with the results in [14,15] for barotropic surface waves. However, from (5.10), the mean level change at the interface can be positive or negative depending on the ratio $h = H_1/H_2$. This is obvious, since the mean momentum transport in the lower layer will induce a positive change of the interfacial level, while the mean momentum transport in the upper layer will lead to a negative change (this is like a surface wave upside down). The difference in density here is negligible, and since $\overline{U}_{S1}/\overline{U}_{S2} = H_2/H_1$, the largest Stokes momentum transport will occur in the upper layer when $H_1 < H_2$. Hence, the interfacial level becomes negative in that case, as seen from (5.10).

6. Particular solutions

The vertically-dependent parts $\overline{u}_{B1}$ and $\overline{u}_{B2}$ of (4.9) and (4.11) yield the mean velocity in the viscous boundary layers at both sides of the interface. We find that

$$\overline{u}_{B1} = \delta^2 C_* Q_1 \left[\frac{3}{4} Q_1 \exp(-2\gamma_1 c) - 2\exp(-\gamma_1 c)\cos(\gamma_1 c)\right] \tag{6.1}$$

$$\overline{u}_{B2} = \delta^2 C_* Q_2 h^2 \left[\frac{3}{4} Q_2 \exp(2\gamma_2 c) - 2\exp(\gamma_2 c)\cos(\gamma_2 c)\right] \tag{6.2}$$

In the shallow-water approximation the Stokes drift source term vanishes on the right-hand sides of the Lagrangian drift equations (4.9) and (4.11); see the discussion in [21] for the viscous one-layer case. To obtain a complete particular solution to this problem, we therefore must add the Stokes drift (5.6) and (5.7) in each layer, respectively. The particular solution to the Lagrangian drift problem then becomes:

$$\overline{u}_{S1} + \overline{u}_{B1} = \overline{u}_{S1}\left[1 + \frac{3}{2} Q_1^2 \exp(-2\gamma_1 c) - 4Q_1 \exp(-\gamma_1 c)\cos(\gamma_1 c)\right], \tag{6.3}$$

$$\overline{u}_{S2} + \overline{u}_{B2} = \overline{u}_{S1} h^2 \left[1 + \frac{3}{2} Q_2^2 \exp(2\gamma_2 c) - 4Q_2 \exp(\gamma_2 c)\cos(\gamma_2 c)\right]. \tag{6.4}$$

Since $\overline{u}_S + \overline{u}_B$ generally does not satisfy the boundary condition for the mean flow at the interface; see [20] for surface waves, an Eulerian current $\overline{u}_E$ will develop, starting at the interface and diffuse upwards and downwards in this problem. The total Lagrangian mean drift velocity $\overline{u}_L$ thus becomes

$$\overline{u}_{L1,2} = \overline{u}_{S1,2} + \overline{u}_{B1,2} + \overline{u}_{E1,2}. \tag{6.5}$$

Assuming that the Eulerian current starts from zero, the initial Lagrangian drift is

$$\overline{u}_{L1,2}(t = 0) = \overline{u}_{S1,2} + \overline{u}_{B1,2}. \tag{6.6}$$

In the notion of [20], where the Lagrangian mean drift is the Stokes drift plus the "Eulerian mean" velocity, the "Eulerian mean" in the present formulation should be understood as

$$\overline{u}_B + \overline{u}_E.$$

7. Eulerian mean flow and VWS

The Eulerian parts of the mean velocities in (4.9) and (4.11) are governed by

$$\overline{u}_{E1cc} - \overline{u}_{E1t}/\nu_1 = 0, \tag{7.1}$$

$$\overline{u}_{E2cc} - \overline{u}_{E2t}/\nu_2 = 0. \tag{7.2}$$

The boundary conditions for this case are obtained from (4.5) and (4.6). Inserting for $\tilde{x}_1$ and $\tilde{x}_2$, we obtain to leading order in γ_1, γ_2:

$$\nu_1 \overline{u}_{L1c} - \nu_2 \overline{u}_{L2c} = 2\overline{u}_{S1}\left[Q_1(1 - Q_1)\nu_1\gamma_1 + Q_2 h^2(1 - Q_2)\nu_2\gamma_2\right], \quad c = 0 \tag{7.3}$$

$$\overline{u}_{L1} = \overline{u}_{L2}, c = 0. \tag{7.4}$$

By utilizing that $\overline{u}_{E1,2} = \overline{u}_{L1,2} - \overline{u}_{S1,2} - \overline{u}_{B1,2}$, (7.3) and (7.4) yield the boundary conditions for the transient mean velocities:

$$\nu_1 \overline{u}_{E1c} - \nu_2 \overline{u}_{E2c} = -\nu_1\gamma_1 \overline{u}_{S1} G, \quad c = 0 \tag{7.5}$$

and

$$\overline{u}_{E1} - \overline{u}_{E2} = -\overline{u}_{S1} F, c = 0. \tag{7.6}$$

The dimensionless parameters F and G are given by

$$F = 1 + \frac{3}{2}Q_1^2 - 4Q_1 - h^2\left(1 + \frac{3}{2}Q_2^2 - 4Q_2\right), \tag{7.7}$$

$$G = Q_1(2 - Q_1) + Q_2(2 - Q_2)h^2\nu_2^{1/2}/\nu_1^{1/2}, \tag{7.8}$$

where Q_1, Q_2 are defined by (A.15). Introducing

$$r = \nu_2^{1/2}/\nu_1^{1/2}, \tag{7.9}$$

F and G in (7.7)–(7.8) can be written

$$F = (1 + h)\left[(3 + r)h - 1 - 3r\right]/(2 + 2r) \tag{7.10}$$

$$G = r(1 + h)^2/(1 + r). \tag{7.11}$$

In (7.5) the left-hand side represents the difference in VWS per unit density across the interface; see e.g. [1] for surface waves. By definition, we write for the VWS in the two layers:

$$\tau_{w1,2}/\rho = \nu_{1,2}\overline{u}_{E1,2c},\ c = 0. \tag{7.12}$$

Using (7.5) and (7.10)–(7.11), we find

$$\tau_{w1}/\rho - \tau_{w2}/\rho = -\omega G\overline{u}_{S1}/(2\gamma_1). \tag{7.13}$$

From (A.23) we note that the spatial attenuation rate can be written

$$\alpha = kG/[4H_1\gamma_1(1 + h)]\,. \tag{7.14}$$

Accordingly, from (7.13):

$$\tau_{w1}/\rho - \tau_{w2}/\rho = -2\alpha C_* H_1(1 + h)\overline{u}_{S1}, \tag{7.15}$$

where C_*, defined by (4.10), is the phase (and group velocity) for long interfacial waves. By introducing the Stokes volume fluxes (5.8) for this problem into (7.15), we finally obtain that

$$\tau_{w1}/\rho - \tau_{w2}/\rho = \left[C_*(\overline{U}_{S1} + \overline{U}_{S2})\right]_a\,. \tag{7.16}$$

This is a fundamental, novel result, relating the VWS's to the divergence of the total horizontal wave momentum flux in a two-layer model. The relation (7.16) should also hold in the case when the interface is covered by a thin film (leading to a larger damping coefficient α of the interfacial wave). A similar result for dispersive surface waves (one deep layer) was derived in [2].

The Eulerian part of this problem, governed by (7.1)–(7.2) and the boundary conditions (7.5)–(7.6), is a transient one. For the ideal case of an infinitely long channel, a final steady solution requires a balance between the viscous bottom stress and the VWS. However, in practice with experiments in a tank of length L, mass will accumulate near the end of the tank due to the wave-induced drift, generating adverse pressure gradients (interfacial/surface tilts) that will cause a return flow in the tank. We have not included such mean gradients in our analysis. Since the drift velocity is typically proportional to the Stokes drift, this puts an upper limit t_{adv} to the duration of the experiment of the order $t_{adv} \sim L/\overline{u}_{S1,2}$ if comparisons with the present theory should be made.

8. Transient solutions

In the present investigation we focus on the transient part of the problem evolving in the vicinity of the interface, and neglect the effects of surface and bottom friction. To illustrate the mean wave momentum transfer to Eulerian currents, we first integrate (7.1) and (7.2) in the vertical. The VWS, defined by (7.12), become

$$\tau_{w1}/\rho = -\int_0^{H_1}\overline{u}_{E1t}dc = -\overline{U}_{E1t}, \tag{8.1}$$

$$\tau_{w2}/\rho = \int_{-H_2}^{0}\overline{u}_{E2t}dc = \overline{U}_{E2t}, \tag{8.2}$$

where $\overline{U}_{E1,2}$ are the Eulerian mean volume transports. By combining (7.16) and (8.1)–(8.2), we obtain that

$$\left[\overline{U}_{E1} + \overline{U}_{E2}\right]_t + \left[C_*(\overline{U}_{S1} + \overline{U}_{S2})\right]_a = 0, \tag{8.3}$$

which constitutes the total horizontal mean momentum conservation in the two-layer system.

To obtain specific solutions for the Eulerian mean flow, we apply Laplace transforms. We take that $\overline{u}_{E1,2}(t = 0) = 0$, and assume that the diffusive solutions have not reached the bottom or the surface in the model, i.e. $\overline{u}_{E1} = 0$ when $c \to \infty$, and $\overline{u}_{E2} = 0$ when $c \to -\infty$. In this way we deliberately limit the validity of our solutions in time to focus on the early development of the drift currents near the interface. Using the boundary conditions (7.5)–(7.6), the solutions can be written in terms of complementary and integrated complementary error functions:

$$\overline{u}_{E1} = -\overline{u}_{S1}R\left[r\mathrm{Ferfc}\left(\frac{c}{2(\nu_1 t)^{1/2}}\right) - G(2\omega t)^{1/2}\mathrm{ierfc}\left(\frac{c}{2(\nu_1 t)^{1/2}}\right)\right],\ c \geq 0, \tag{8.4}$$

$$\overline{u}_{E2} = \overline{u}_{S1}R\left[F\mathrm{erfc}\left(-\frac{c}{2(\nu_2 t)^{1/2}}\right) + G(2\omega t)^{1/2}\mathrm{ierfc}\left(-\frac{c}{2(\nu_2 t)^{1/2}}\right)\right],\ c \leq 0, \tag{8.5}$$

where F and G are given by (7.10)–(7.11). Furthermore, $r = \nu_2^{1/2}/\nu_1^{1/2} = \gamma_1/\gamma_2$, and $R = 1/(1 + r)$.

From (7.16) we notice that the difference between the VWS's is independent of time, while for the ratio we obtain from (8.4)–(8.5):

$$\tau_{w1}/\tau_{w2} = \left[F - (\pi/r)(t/T)^{1/2}G\right]/\left[F + \pi(t/T)^{1/2}G\right], \tag{8.6}$$

where T is the wave period. A negative value on the right-hand side of (8.6) less than minus one means that the time derivative of the total horizontal Eulerian mean momentum in the upper layer is larger than the corresponding one the lower layer. For longer times we note that $\tau_{w1}/\tau_{w2} \to -1/r$. Hence, if $r < 1$, i.e. more viscous fluid on top, the Eulerian drift velocity will increase fastest in the upper layer. More generally, from (7.10)–(7.11) we notice that $G > 0$ for all possible choice of parameters, while $F = 0$ when $h = (1 + 3r)/(3 + r)$. Accordingly, when $h < (1 + 3r)/(3 + r)$, we have $F < 0$. In this case with $r < 1$, (more viscous on top) we have from (8.6) that $|\tau_{w1}/\tau_{w2}| > 1$ when $t > 0$. If the fluid on top is much more viscous than the lower fluid ($r \ll 1$), this will happen for all $h = H_1/H_2 < 1/3$. We will elaborate more on the momentum transfer in the case studies presented in Section 9. Again, we emphasize that our approach yielding solutions which grow in time, is only valid for relatively small times. The asymptotic solutions for long times will equilibrate due to the effect of friction in the same manner as the surface wave drift in a shallow single layer [20].

9. Case studies

The obvious starting point for a discussion on how viscosity variations and layer depth ratios influence the Lagrangian drift solution $\overline{u}_{L1,2} = \overline{u}_{S1,2} + \overline{u}_{B1,2} + \overline{u}_{E1,2}$ is the symmetric case $\nu_1 = \nu_2 = \nu$, and $H_1 = H_2$, i.e. $r = 1, h = 1$. Then $R = 1/2$, $F = 0$, and $G = 2$ in (8.4)–(8.5). In Fig. 1, we have depicted the non-dimensional Lagrangian solution $\overline{u}_L/\overline{u}_{S1} = (\overline{u}_S + \overline{u}_B + \overline{u}_E)/\overline{u}_{S1}$ in the two layers when $\gamma_1 H_1 = \gamma_2 H_1 = 1000$.

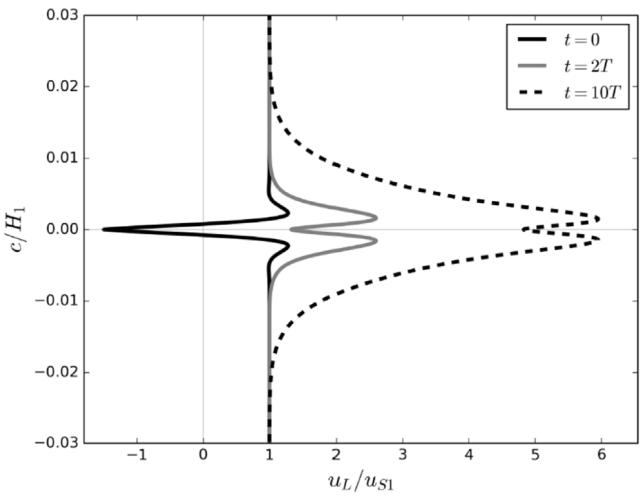

Fig. 1. Non-dimensional Lagrangian drift $\overline{u}_L/\overline{u}_{S1}$ when $t = 0$ (black line), $t = 2T$ (gray line), and $t = 10T$ (dashed line) in the two layers as function of the non-dimensional depth coordinate c/H_1. Here $h = 1$, and $\gamma_1 H_1 = \gamma_2 H_1 = 1000$.

The flow is symmetric about the interface. This is obvious, since from (8.6), $\tau_{w1}/\tau_{w2} = -1$ for all times in this problem. Initially, the drift is negative (backward) at the interface; see the black curve in Fig. 1. However, the induced Eulerian mean flow very quickly changes this picture. At the surface when $t > 0$, we find from (8.4)–(8.5) for this case:

$$\overline{u}_{E1}(c = 0) = \overline{u}_{E2}(c = 0) = \overline{u}_{S1}(4t/T)^{1/2}. \tag{9.1}$$

When this velocity is added to the initial flow, we realize that the Lagrangian drift at the interface is quite rapidly accelerated, and will become positive after a few wave periods, as seen in Fig. 1. Dore, in a series of papers [6–9] was the first to show that time-independent Eulerian mean currents in undamped interfacial waves were much larger than for surface waves with a clean surface.

It is the large VWS's that cause the rapid growth of the Eulerian current in this case. We find at $c = 0$:

$$\tau_{w1}/(\rho\nu) = \overline{u}_{E1c} = -\gamma\overline{u}_{S1}, \tag{9.2}$$

$$\tau_{w2}/(\rho\nu) = \overline{u}_{E2c} = \gamma\overline{u}_{S1}. \tag{9.3}$$

These VWS's are in fact similar to that found for short progressive gravity waves in the presence of an inextensible surface film [2], and shown in [3] to explain quite well the transient drift of plastic sheets in the laboratory experiments reported in [22]. For the pioneering work on surface wave drift in the presence of an inextensible film, we refer to Craik [4]. It was in fact Craik that also pointed out the similarity between the inextensible surface film case and the interfacial wave case. We demonstrate here explicitly that this enhancement is related to the strong VWS's that appear in interfacial waves with a clean interface.

A change of the viscosity in the upper (or lower) layer alters this picture. We consider here the case when the viscosity is increasing in the upper fluid, while keeping $H_1 = H_2$. The effect of increasing viscosity is seen in Fig. 2a and b.

We note from the figure that the total Eulerian momentum in the upper layer increases more than in the lower layer as $r = \gamma_1/\gamma_2$ becomes smaller. In fact, after $t = 10T$ (dashed lines), we find that in (a): $\tau_{w1}/\tau_{w2} = -1.86$, and in (b): $\tau_{w1}/\tau_{w2} = -6.57$, which underlines this point.

The changes of the drift currents due to depth ratio variations are less dramatic than for viscosity changes. In Fig. 3 we have depicted the non-dimensional Lagrangian solution $\overline{u}_L/\overline{u}_{S1}$ in the two layers for two values of h when $\nu_1 = \nu_2$.

In this case, after $t = 10T$ (dashed lines), we find that in (a): $\tau_{w1}/\tau_{w2} = -1.22$, and in (b): $\tau_{w1}/\tau_{w2} = -1.4$, illustrating the relatively slow growth in upper layer momentum compared to lower layer momentum as H_2 increases.

In a field situation one may find a very viscous thin layer above a much deeper and less viscous layer (e.g. near-shore oil spills). In Fig. 4 we have depicted the non-dimensional Lagrangian solution $\overline{u}_L/\overline{u}_{S1}$ in the two layers for such a case.

In this example we find that $\tau_{w1}/\tau_{w2} = -19.1$ after $t = 10T$, illustrating the strong growth of upper layer momentum for this configuration. In such cases the Lagrangian drift in the deep lower layer will be negligible, and the increase in drift velocity (above the Stokes drift) will be observed in the growing diffusive layer on the more viscous side of the interface.

10. Suggestion for a simple laboratory verification of the theory

To test the theory developed here experimentally, one could use olive oil and water as working fluids. At room temperature we have for olive oil that $\rho_1 = 911$ kg m^{-3} and $\nu_1 = 9.22 \times 10^{-5}$m^2 s^{-1}, while for water $\rho_2 = 1000$ kg m^{-3} and $\nu_2 =$

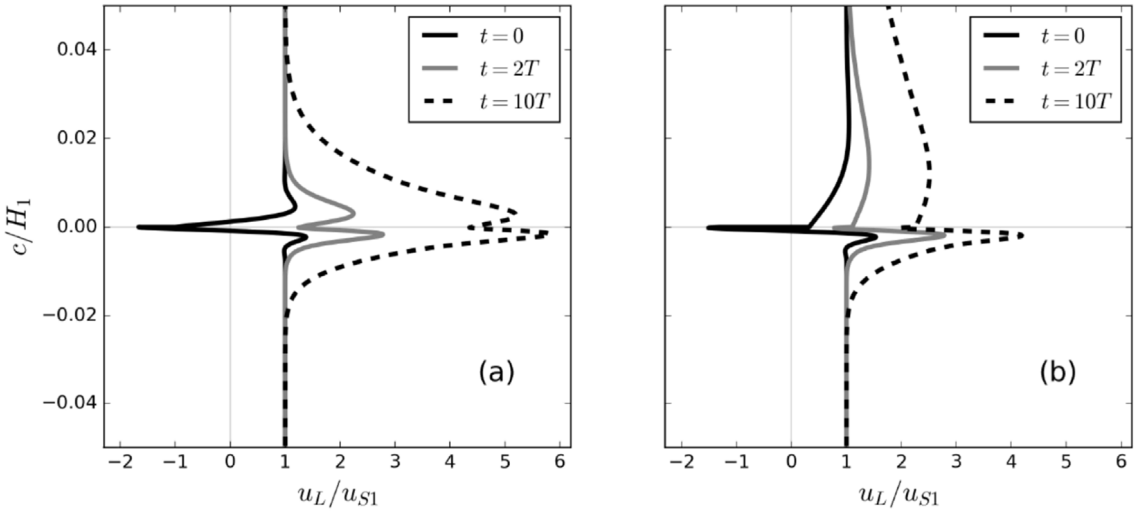

Fig. 2. Text as in Fig. 1 with $h = 1$. Here (a): $\gamma_1 H_1 = 500$, $\gamma_2 H_1 = 1000$, (b): $\gamma_1 H_1 = 100$, $\gamma_2 H_1 = 1000$.

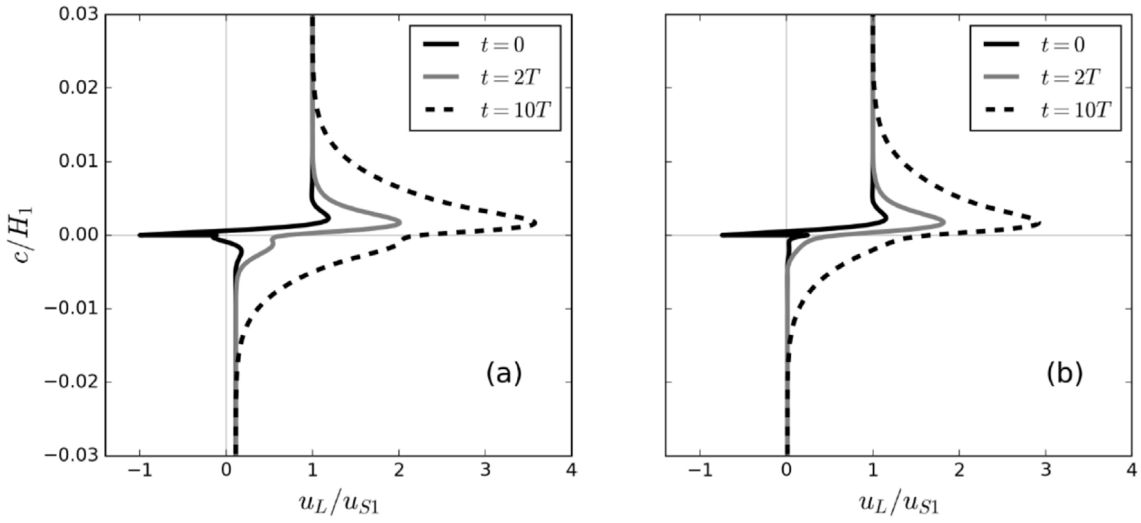

Fig. 3. Text as in Fig. 1, with $\gamma_1 H_1 = \gamma_2 H_1 = 1000$. Here (a): $h = 1/3$, (b): $h = 1/10$.

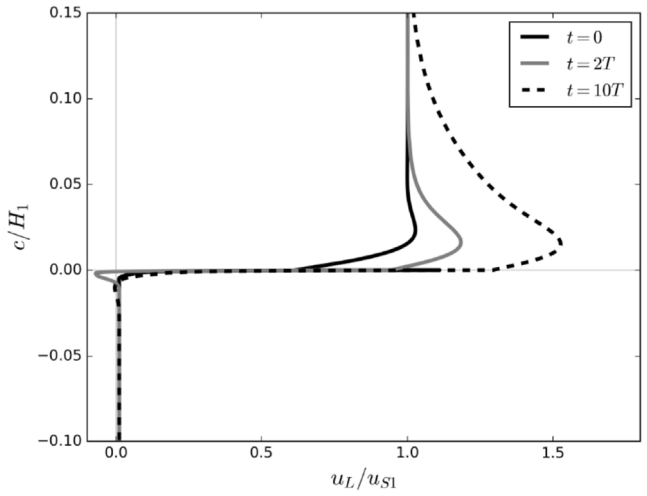

Fig. 4. Text as in Fig. 1. Here $h = 1/10$, $\gamma_1 H_1 = 100$, and $\gamma_2 H_1 = 1000$.

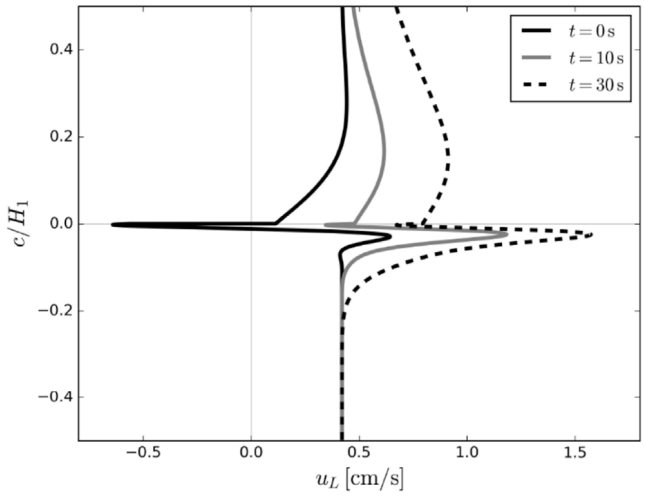

Fig. 5. Dimensional Lagrangian drift $\overline{u}_L$ when $t = 0$ (black line), $t = 10$ s (gray line), and $t = 30$ s (dashed line) in the two layers as function of the non-dimensional depth coordinate c/H_1. Here $H_1 = H_2 = 0.1$ m, $\lambda = 1$ m, $\nu_1 = 9.22 \times 10^{-5}$ m^2 s^{-1} (olive oil), and $\nu_2 = 1.12 \times 10^{-6}$ m^2 s^{-1} (water).

1.12×10^{-6} m^2 s^{-1}. The reduced gravity in this case becomes $g_* = 0.87$ m s^{-2}. With $H_1 = H_2 = 0.1$ m, and a wavelength $\lambda = 1$ m, we find that $C_* = 0.21$ m s^{-1}, and $T = 4.8$ s. Furthermore, in this case $\gamma_1 H_1 = 8.4$ and $\gamma_2 H_2 = 76.6$. The parameter values in this example fulfill the assumptions behind our analysis quite well, i.e. $\lambda \gg H_1, H_2$ (long waves) and $\gamma_1 H_1, \gamma_2 H_2 \gg 1$ (thin Stokes layers). A reasonable interfacial wave amplitude in this experiment is $A = 2$ cm. Then the expansion parameter becomes $\varepsilon = A/H_1 = 0.2$. From (A.11)–(A.12) we obtain for the inviscid part of the wave field that the maximum horizontal velocity jump across the interface is $\Delta\tilde{u} = 8.2$ cm s^{-1}. The bulk Richardson number for the wave problem can be defined as

$$\mathrm{Ri} = g_* H_1/(\Delta\tilde{u})^2. \tag{10.1}$$

With our adopted values we find that Ri $= 12.9$, so the basic configuration is definitely stable. In this example the maximum Stokes drift from (5.6)–(5.7) becomes $\overline{u}_S = 0.42$ cm s^{-1} in both layers. With $|\tilde{u}|_{max} = 4.1$ cm s^{-1} and $C_* = 21$ cm s^{-1}, we notice that the basic condition for the validity of our perturbation analysis, i.e. $|\overline{u}_S|_{max} \ll |\tilde{u}|_{max} \ll C_*$, is reasonably well fulfilled.

In Fig. 5 we have depicted the dimensional Lagrangian solution $\overline{u}_L$ in the two layers for this particular case.

After about 6 wave periods we note from Fig. 5 (dashed line) that the drift velocity near the interface in the upper layer is about 1 cm s^{-1}, while in the lower layer the drift velocity close to the interface is 1.7 cm s^{-1}. These drift velocities, and velocity differences, should easily be detected by applying a common Particle Image Velocimetry (PIV) flow visualization technique.

11. Discussion and concluding remarks

For long interfacial waves in a two-layer system of immiscible fluids the inviscid Stokes drift is positive (in the direction of the wave propagation) in both layers. However, the initial drift (inviscid Stokes drift + viscous boundary-layer terms) associated with the instantaneously imposed wave field does not generally fulfill the conditions at the common boundary. Here the initial drift may also be negative. As a consequence, transient Eulerian mean currents develop on both sides of the interface to ensure continuity of velocities and viscous stresses. The VWS here plays a crucial part, transferring lost wave momentum due to damping into Eulerian mean currents; see e.g. [1] for surface waves. In

general, the transient Eulerian current driven by the VWS tends to promote positive drift at the interface as time increases. It is found that the strong VWS in interfacial waves is similar to that enhancing the drift in short surface waves in the presence of surface films; see e.g. [3]. A new relation is derived that shows that the difference between the VWS's at the interface is given by the divergence of the total horizontal wave momentum flux in a two-layer system.

Reduced gravity models for interfacial long waves have successfully been applied to model the first baroclinic response in a continuously stratified system with a pronounced pycnocline; see e.g. [23,24]. However, by assuming a discontinuity in density between the two layers of miscible fluids (such as warm water above cold water), the backward Stokes drift velocity for the first baroclinic mode near the peak of the Brunt-Väisälä frequency is not reproduced; see [25] for constant Brunt-Väisälä frequency N, [26] in the case of a thin thermocline with constant N, and [27] for internal equatorial Kelvin waves with arbitrary stable stratification. In the two-layer miscible case we must on theoretical grounds postulate a delta-function type negative Stokes drift at the interface in order to comply with the requirement of zero horizontal Stokes volume transport for each internal mode [27]. This is definitely unphysical, and in practice, a pycnocline will always develop between miscible layers due to instabilities and turbulent mixing.

In the case of immiscible fluid layers treated here the initial Lagrangian transport only get small negative boundary-layer contributions of $O(1/\gamma_1, 1/\gamma_2)$ to the positive Stokes transport in each layer. At later times the Lagrangian transport in the growing boundary layers at both sides of the interface is entirely positive. Hence, the total Lagrangian transport in the immiscible case is positive.

In a laboratory experiment with a two-layer model we will also find enhancement of the mean drift in the surface boundary layer, and in the bottom boundary layer. These layers are much thinner than the layer depths H_1, H_2, and for times related to the duration of a wave tank experiment (before the build-up of mean pressure gradients occurs), the drift solutions near the surface and the bottom will not interfere with the Lagrangian mean currents at the interface studied in this paper. The need for time in developing friction-induced currents at the surface, interface and at the bottom is clearly seen from the study of large-amplitude interfacial solitons [28], where there is excellent agreement between measurements and inviscid theory.

Apart from the obvious environmental aspects, one of the motivations behind this theoretical research has been to inspire keen experimentalists to work on waves in a two-layer system with immiscible fluids. Albeit the Stokes drift is not easy to measure in wave tanks, recent progress is very promising; see e.g. the discussion in [29] and the experiments in [5]. Hence, the present results of rapidly increasing drift currents near the interface should be possible to capture in the laboratory.

Acknowledgments

Financial support from the Research Council of Norway through the Grant 280625 (Dynamics of floating ice), and Grant 244262 (RETROSPECT) are gratefully acknowledged.

Appendix. The linear baroclinic response

We here define linear quantities (with a tilde) as $\tilde{x}_{1,2} = \varepsilon x^{(1)}_{1,2}, \tilde{z}_{1,2} = \varepsilon z^{(1)}_{1,2}, \tilde{\eta} = \varepsilon\eta^{(1)}, \tilde{\xi} = \varepsilon\xi^{(1)}$, and $\tilde{u}_1 = \tilde{x}_{1t}, \tilde{u}_2 = \tilde{x}_{2t}$. The equations to $O(\varepsilon)$become from (3.9) and (3.10):

$$\nu_1\tilde{u}_{1cc} - \tilde{u}_{1t} = g\tilde{\eta}_a \tag{A.1}$$

$$\nu_2\tilde{u}_{2cc} - \tilde{u}_{2t} = g_*\tilde{\xi}_a + g\tilde{\eta}_a \tag{A.2}$$

From volume conservation:

$$\tilde{x}_{1,2a} + \tilde{z}_{1,2c} = 0 \tag{A.3}$$

Hence

$$\tilde{\eta} - \tilde{\xi} = -\int_0^{H_1} \tilde{x}_{1a}dc \tag{A.4}$$

$$\tilde{\xi} = -\int_{-H_2}^{0} \tilde{x}_{2a}dc \tag{A.5}$$

which is just the linearized version of (2.6)–(2.7). The focus in this paper is on the baroclinic response, i.e. we assume that

$$\left|\tilde{\xi}\right| \gg |\tilde{\eta}| \tag{A.6}$$

Utilizing (A.6), one obtains from (A.4)–(A.5) that the volume fluxes in each layer are equal in magnitude and oppositely directed. Integrating (A.1)–(A.2) over the respective fluid layer depths, and assuming free-slip conditions at the surface and the bottom, one obtains by adding the linearized fluxes:

$$\tilde{\eta} = -(\Delta\rho/\rho)H_2\tilde{\xi}/(H_1 + H_2) \tag{A.7}$$

The linearized governing equations then become from (A.1)–(A.2):

$$\nu_1\tilde{u}_{1cc} - \tilde{u}_{1t} = -g_*H_2\tilde{\xi}_a/(H_1 + H_2) \tag{A.8}$$

$$\nu_2\tilde{u}_{2cc} - \tilde{u}_{2t} = g_*H_1\tilde{\xi}_a/(H_1 + H_2) \tag{A.9}$$

In this problem we take that the $O(\varepsilon)$ interfacial displacement can be written in complex form as

$$\tilde{\xi} = \varepsilon H_1 e^{i(\kappa a - \omega t)}, \tag{A.10}$$

where ω is the real frequency, and $\kappa = k + i\alpha$. Here k is the real wave number and α is the spatial wave attenuation coefficient due to friction. By assuming continuity of horizontal velocities and viscous stresses at the interface, we readily obtain from (A.8)–(A.9):

$$\tilde{x}_1 = -\frac{i\kappa g_*H_1H_2}{\omega^2\,(H_1 + H_2)}\varepsilon\,[1 - Q_1 \times \exp\left(-(1-i)\,\gamma_1 c\right)]\exp(i\,(\kappa a - \omega t)), \tag{A.11}$$

$$\tilde{x}_2 = \frac{i\kappa g_*H_1^2}{\omega^2\,(H_1 + H_2)}\varepsilon\,[1 - Q_2\exp\left((1-i)\,\gamma_2 c\right)]\exp(i\,(\kappa a - \omega t)). \tag{A.12}$$

Here

$$\gamma_1 = [\omega/(2\nu_1)]^{1/2}\,,\ \gamma_2 = [\omega/(2\nu_2)]^{1/2} \tag{A.13}$$

are the inverse boundary-layer thicknesses on both sides of the interface. In the literature $1/\gamma_1$ and $1/\gamma_2$ are often referred as the Stokes boundary-layer thicknesses. The present analysis assumes that the Stokes boundary layers are thin, i.e. that

$$\gamma_1H_1 \gg 1,\ \gamma_2H_2 \gg 1. \tag{A.14}$$

Furthermore, in (A.11)–(A.12), we have defined

$$Q_1 = (H_1 + H_2)(1 - R)/H_2,\ Q_2 = (H_1 + H_2)R/H_1 \tag{A.15}$$

where

$$R = \nu_1^{1/2}/(\nu_1^{1/2} + \nu_2^{1/2}) < 1. \tag{A.16}$$

The kinematic boundary conditions at the surface and the bottom for the baroclinic mode are:

$$\tilde{z}_1 = -\frac{g_*H_2}{g(H_1 + H_2)}\tilde{\xi},\quad c = H_1, \tag{A.17}$$

$$\tilde{z}_2 = 0, \quad c = -H_2. \tag{A.18}$$

Hence, from (A.3):

$$\tilde{z}_1 = \frac{\kappa^2 g_* H_1^2 H_2}{\omega^2 (H_1 + H_2)} \varepsilon \left[1 - c/H_1 - \frac{(1+i)Q_1}{2\gamma_1 H_1} \exp(-(1-i)\gamma_1 c) \right] \times \exp(i(\kappa a - \omega t)) - \frac{g_* H_1 H_2}{g\,(H_1 + H_2)} \varepsilon \exp(i(\kappa a - \omega t)), \tag{A.19}$$

$$\tilde{z}_2 = \frac{\kappa^2 g_* H_1^2 H_2}{\omega^2 (H_1 + H_2)} \varepsilon \left[1 + c/H_2 - \frac{(1+i)Q_2}{2\gamma_2 H_2} \exp((1-i)\gamma_2 c) \right] \times \exp(i(\kappa a - \omega t)). \tag{A.20}$$

It is easily demonstrated from the definitions (A.15) and (A.16) that $Q_1/(\gamma_1 H_1) = Q_2/(\gamma_2 H_2)$ in (A.19)–(A.20). Accordingly, when we neglect the small contribution from the surface, we have that $\tilde{z}_1 = \tilde{z}_2$ at $c = 0$. The remaining kinematic condition at the interface is

$$\tilde{\xi} = \tilde{z}_1, \quad c = 0. \tag{A.21}$$

Utilizing (A.6) and (A.10) in (A.21), we obtain the complex dispersion relation

$$\omega^2 = \frac{\kappa^2 g_* H_1 H_2}{H_1 + H_2} \left[1 - \frac{(1+i)Q_1}{2\gamma_1 H_1} \right]. \tag{A.22}$$

From the real part of (A.22), we find to lowest order

$$\omega^2 = \frac{g_* H_1 H_2}{H_1 + H_2} k^2, \tag{A.23}$$

while the imaginary part yields the spatial damping rate

$$\alpha = \frac{H_1 + H_2}{4 H_1 H_2 (\gamma_1 + \gamma_2)} k. \tag{A.24}$$

In this problem we have assumed that $\alpha/k \ll 1$.

References

[1] M.S. Longuet-Higgins, A nonlinear mechanism for the generation of sea waves, Proc. Roy. Soc. A 311 (1969) 371–389.
[2] J.E. Weber, Virtual wave stress and mean drift in spatially damped surface waves, J. Geophys. Res. 106 (2001) 11,653–11,657.
[3] K.H. Christensen, J.E. Weber, Drift of an inextensible sheet caused by surface waves, Environ. Fluid Mech. 5 (2005) 492–505.
[4] A.D.D. Craik, The drift in water waves, J. Fluid Mech. 116 (1982) 187–205.
[5] J. Grue, J. Kolaas, Experimental particle paths and drift velocity in steep waves at finite water depth, J. Fluid Mech. 810 (2017) R1, http://dx.doi.org/10.1017/jfm.2016.726.
[6] B.D. Dore, Mass transport in a layered fluid system, J. Fluid Mech. 40 (1970) 113–126.
[7] B.D. Dore, On mass transport induced by interfacial oscillations at a single frequency, Proc. Camb. Phil. Soc. 74 (1973) 333–347.
[8] B.D. Dore, Some effects of the air-water interface on gravity waves, Geophys. Astrophys. Fluid Dyn. 10 (1978) 215–230.
[9] B.D. Dore, A double boundary-layer model of mass transport in progressive interfacial waves, J. Engrg. Math. 12 (1978) 289–301.
[10] J. Wen, P.L.-F. Liu, Mass transport of interfacial waves in two-layer fluid system, J. Fluid Mech. 297 (1995) 231–254.
[11] J.E. Weber, E. Førland, Effect of air on the drift velocity of water waves, J. Fluid Mech. 218 (1990) 619–640.
[12] I. Piedra-Cueva, Drift velocity of spatially decaying waves in a two-layer viscous system, J. Fluid Mech. 299 (1995) 217–239.
[13] C.-O. Ng, Mass transport and set-ups due to partial standing surface waves in a two-layer viscous system, J. Fluid Mech. 520 (2004) 297–325.
[14] M.S. Longuet-Higgins, Eulerian and Lagrangian aspects of surface waves, J. Fluid Mech. 173 (1986) 683–707.
[15] M.E. McIntyre, A note on the divergence effect and the Lagrangian-mean surface elevation in periodic water waves, J. Fluid Mech. 189 (1988) 235–242.
[16] H. Lamb, Hydrodynamics, sixth ed., Cambridge University Press, Cambridge, U.K., 1932.
[17] W.J. Pierson, Perturbation analysis of the Navier–Stokes equations in Lagrangian form with selected solutions, J. Geophys. Res. 67 (1962) 3151–3160.
[18] D. Clamond, On the Lagrangian description of steady surface gravity waves, J. Fluid Mech. 589 (2007) 433–454.
[19] G.G. Stokes, On the theory of oscillatory waves, Trans. Camb. Phil. Soc. 8 (1847) 441–455.
[20] M.S. Longuet-Higgins, Mass transport in water waves, Phil. Trans. Roy. Soc. Lond. A 245 (1953) 535–581.
[21] J.E. Weber, Lagrangian studies of wave-induced flows in a viscous ocean, Deep-Sea Res. Part II 160 (2019) 68–81.
[22] A.W.K. Law, Wave-induced surface drift of an inextensible thin film, Ocean Eng. 26 (1999) 1145–1168.
[23] J. McCreary, Eastern tropical ocean response to changing wind systems: With application to El Niño, J. Phys. Oceanogr. 6 (1976) 632–645.
[24] A.J. Busalacchi, J.J. O'Brien, The seasonal variability in a model of the tropical Pacific, J. Phys. Oceanogr. 10 (1980) 1929–1951.
[25] C. Wunsch, On the mean drift in large lakes, Limnol. Oceanogr. 18 (1973) 793–795.
[26] M.A. Al-Zanaidi, B.D. Dore, Some aspects of internal wave motions, Pure Appl. Geophys. 114 (1976) 403–414.
[27] J.E. Weber, K.H. Christensen, G. Broström, Stokes drift in internal equatorial kelvin waves: Continuous stratification versus two-layer models, J. Phys. Oceanogr. 44 (2014) 591–599.
[28] J. Grue, A. Jensen, P.-O. Rusås, J.K. Sveen, Properties of large-amplitude internal waves, J. Fluid Mech. 380 (1999) 257–278.
[29] T.S. van den Bremer, Ø. Breivik, Stokes drift, Phil. Trans. R. Soc. A 376 (2017) 20170104.